

Prediction of stiffener buckling in press bend forming of integral panels

YAN Yu¹, WANG Hai-bo¹, WAN Min²

1. College of Mechanical and Electrical Engineering, North China University of Technology, Beijing 100144, China;

2. School of Mechanical Engineering and Automation, Beihang University, Beijing 100191, China

Received 25 October 2010; accepted 14 February 2011

Abstract: In order to predict the buckling of stiffeners in the press bend forming of the integral panel, a method for solving the critical buckling load of the stiffeners in press bend forming process was proposed based on energy method, elastic-plastic mechanics and numerical analysis. Bend to buckle experiments were carried out on the designed press bend dies. It is found that the predicted results based on the proposed method agree well with the experimental results. With the proposed method, the buckling of the stiffeners in press bend forming of the aluminum alloy integral panels with high-stiffener can be predicted reasonably.

Key words: press bend forming; buckling prediction; integral panel

1 Introduction

Because of the light weight, high stiffness and high structural efficiency, aluminum alloy integral panels with high-stiffener are widely used in modern aircrafts. Press bend forming is an important way to manufacture integral panels, which has many advantages such as low tooling cost, short cycle time and adaptability to different contours [1–3]. Buckling is a severe forming defect in press bend forming process, and its occurrence may lead to great loss [4]. It is well known that the problem resolution relies heavily on experience and involves repeated trial-and-errors in practice. Therefore, how to predict this phenomenon rapidly and accurately has become one of the key problems urgently to be solved for in development of this process. There have been some researches on buckling in aircraft integral panels. YORK and WILLIAMS [5] presented a comparison of exact and approximate methods for the determination of critical buckling loads of prismatic benchmark metal and composite panels. GAL et al [6] presented the buckling analysis of a laboratory tested composite panel under axial compression by means of a simple shell finite element. MATTHIAS and PETER [7] analyzed the critical buckling loads and the postbuckling behaviour with experimental and numerical results of a stiffened panel of aircrafts. DEGENHARDT et al [8] carried out

the finite element analysis of the pre- and post-buckling behavior of the aircraft panels with Abaqus finite element software. However, up to now, literature on the studies of buckling in the press bend forming of integral panels has been scant. LIU [9] and REN et al [10] carried out some experimental and numerical simulation studies on press bend forming to analyze the buckling phenomenon on the stiffeners. The simulation showed the buckling at the same position as the press bend experiment, but it did not provide a quantitative prediction method based on the buckling theory.

Buckling is the behavior that a structure or a structural member deforms in a manner where compressive stresses nonlinearly interact with deflections to produce a non-trivial response of the structure. The critical buckling condition expression can be solved with analytical or numerical method [11]. Energy variation method based on the energy principle of equilibrium stability is the basic method, among which the Galerkin's method (based on the Virtual work principle), the Rayleigh-Ritz method (based on the principle of minimum potential energy) and the Timoshenko method (based on the energy characteristic values of the critical condition) are the common methods [11–15].

Because of the complexity of the integral panel structure, the initial defect of the material, the stress state and the deformation mode, the study of the buckling in press bend forming needs to consider the specific

characteristics of this forming process and combine the analytical analysis based on elasto-plasticity stability theory together with the deformation process in the press bend experiments.

The objective of this study is to propose a prediction method for the buckling of the stiffener based on energy method and numerical analysis. The specimen with I-stiffener was taken as an example and the analytical critical condition was compared with experimental result. Further more, the method was extended to the buckling prediction of the specimens with other multi-stiffener, which lays solid foundation for improving the properties of aircraft integral panels and prolonging the working life of aircrafts.

2 Press bend experiment

Two single stiffener specimens with I-stiffener and T-stiffener respectively and a specimen with multi-stiffener (crosswise stiffened specimen) were designed with reference to typical structures of airplane integral panels. The dimensions of the cross sections are shown in Fig. 1. The lengths of the single stiffener specimen and the specimen with multi-stiffener were 500 and 300 mm, respectively. The material used in this experiment was 7B04-T7451 aluminum alloy which was widely used on the manufacturing of the integral panels. The mechanical properties of 7B04-T7451 aluminum alloy are listed in Table 1.

In order to carry out the experimental research of

Table 1 Mechanical properties of 7B04-T7451 aluminum sheet

Elastic modulus/ GPa	Poisson ratio	Yield strength/ MPa	Strength limit/ MPa	Hardenig coefficient/ MPa	Hardenig exponent
69	0.33	445	558.538	1220.21	0.86

the press bending of integral panel specimens, a set of press bending dies was designed. The punch and the die inserts could be replaced to obtain different bending radii, and the die gap could be changed freely. The dies were installed on a universal triaxial loading test machine. The maximum load of the cylinder was 100 kN, and the maximum vertical displacement was 300 mm.

Press bend experiments were carried out on the press bend experimental set-up. The punch went down until the stiffener buckled. The T-stiffener specimen fractured before buckling, so the other three specimens were mainly focused on the buckling prediction study.

The buckled specimen with I-stiffener and the crosswise stiffened specimen in press bend experiments are shown in Fig. 2.

3 Theoretical analysis of buckling in press bend forming

3.1 Critical buckling load of specimen with I-stiffener

First, the specimen with I-stiffener is taken as an example, the schematic diagram of force analysis of any part of the specimen is shown in Fig. 3. It can be seen

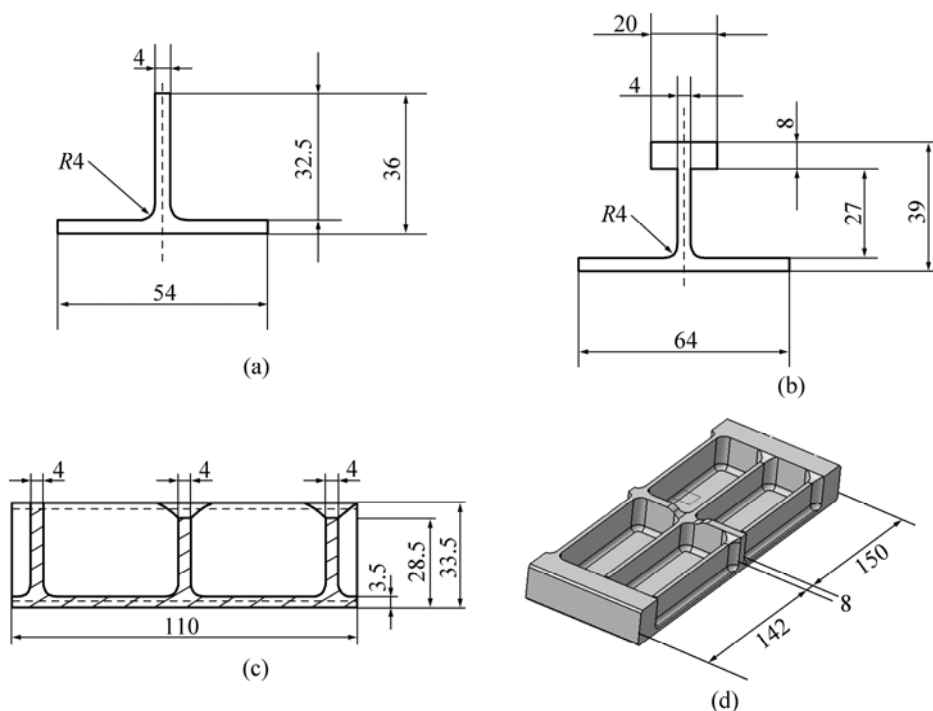


Fig. 1 Dimensions of specimens: (a) Specimen with I-stiffener; (b) Specimen with T-stiffener; (c) Crosswise stiffened specimen; (d) 3D model of crosswise stiffened specimen (unit: mm)

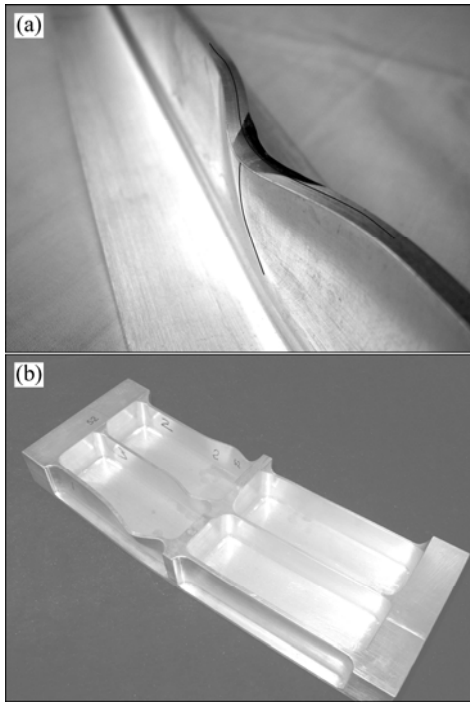


Fig. 2 Photos of buckled specimens in press bend experiments: (a) Buckled specimen with I-stiffener; (b) Buckled crosswise stiffened specimen

that a centralized load is applied to the stiffener top and the two end faces are subjected to normal stress and shear stress, respectively. In the press bend process, the centralized load, normal stress and shear stress increase with the lowering of the punch. The stiffener buckles when the comprehensive effect of the punch load and the corresponding stress on the end faces reaches a critical value.

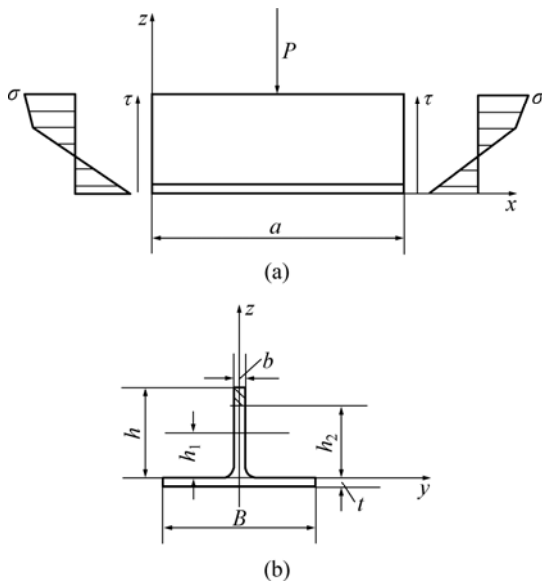


Fig. 3 Schematic diagram of stress analysis of specimen with I-stiffener under press bend forming: (a) Assumed section that buckles first on whole stiffener; (b) Cross section of I-stiffener

For simplicity, the boundaries of the two end faces of buckled section are simplified as simple boundaries, the boundary of the joint section between the stiffener and the skin is simplified as clamped boundary, and the boundary of the stiffener top is unconstrained.

The buckled specimen is shown in Fig. 2(a). Half wave is formed in the length direction meanwhile one quarter of wave is formed in the altitude direction. The peak of the wave in the length direction is formed at the position where the punch contacts the stiffener. Therefore, the deflection equation is expressed with a double trigonometric series as:

$$\omega = f \sin \frac{x\pi}{a} (1 - \cos \frac{z\pi}{h}) \tag{1}$$

The internal energy of the stiffener is expressed as [11, 16]:

$$V_{total} = \frac{1}{2} \int_0^a \int_0^h \int_{-b/2}^{b/2} (\sigma_{xx}\epsilon_{xx} + \sigma_{zz}\epsilon_{zz} + \tau_{xz}\gamma_{xz}) dx dz dy \tag{2}$$

where

$$\begin{cases} \epsilon_{xx} = -y \frac{\partial^2 \omega}{\partial x^2} \\ \epsilon_{zz} = -y \frac{\partial^2 \omega}{\partial z^2} \\ \gamma_{xz} = -2y \frac{\partial^2 \omega}{\partial x \partial z} \end{cases} \tag{3}$$

Both the deformation and the buckling of the stiffener are assumed elastic. According to the generalized Hook law, the relation of the stress and strain is expressed as:

$$\begin{cases} \epsilon_{xx} = \frac{1}{E} (\sigma_{xx} - \nu \sigma_{zz}) \\ \epsilon_{zz} = \frac{1}{E} (\sigma_{zz} - \nu \sigma_{xx}) \\ \gamma_{xz} = \frac{1}{G} \sigma_{xz} \end{cases} \tag{4}$$

where E is the elastic modulus; $G = \frac{E}{2(1+\nu)}$ is the shearing modulus; ν is Poisson ratio.

From Eqs. (2)–(4), the total internal energy of the stiffener is obtained as:

$$V_{Total} = \frac{D}{2} \int_0^a \int_0^h \left\{ (\nabla^2 \omega)^2 - 2(1-\nu) \left[\frac{\partial^2 \omega}{\partial x^2} \frac{\partial^2 \omega}{\partial z^2} - \left(\frac{\partial^2 \omega}{\partial x \partial z} \right)^2 \right] \right\} dx dz \tag{5}$$

where $\nabla^2 = \frac{\partial^2}{\partial x^2} + \frac{\partial^2}{\partial z^2}$ and $D = \frac{Eb^3}{12(1-\nu^2)}$.

The unit length load on the end faces along z (in Fig. 3) is assumed as:

$$N_x = N_0 \left(\frac{z}{h_1} - 1 \right) \quad (6)$$

where N_0 is a constant and h_1 is the coordinate of the central layer in z direction. The work of the normal stress on the two faces is

$$U_{\text{normal}} = \frac{1}{2} N_x \int_0^a \int_0^h \left(\frac{\partial \omega}{\partial x} \right)^2 dx dz \quad (7)$$

The unit length shearing load on the two end faces is set as N_{xz} , then the work of the shearing stress is

$$U_{\text{shear}} = N_{xz} \int_0^a \int_0^h \frac{\partial \omega}{\partial x} \frac{\partial \omega}{\partial z} dx dz \quad (8)$$

The location where load P applied to the stiffener top is $x = \frac{a}{2}$ and the work of load P is

$$U_P = \frac{P}{2} \int_0^h \left(\frac{\partial \omega}{\partial z} \right)_{x=\frac{a}{2}} dz \quad (9)$$

The total work of the external load (stress) is

$$U_{\text{total}} = U_{\text{normal}} + U_{\text{shear}} + U_P \quad (10)$$

From the equilibrium equation of the force on the end faces of the stiffener, it is obtained

$$N_{xy} h = P/2 \quad (11)$$

and

$$\int_0^h N_x z dz + \int_{-t}^0 |z| \frac{N_x B}{b} dz = \frac{P(L-a)}{A} \quad (12)$$

where A is the area of the cross section in specimen.

The buckling problem is solved with energy method. According to the energy method [16], when the total work of the external load is less than that of the total internal energy, the stiffener is in the equilibrium state. The stiffener buckles when the total work of the external load is greater than that of the total internal energy. Therefore, the external load achieves a critical value when $U_{\text{total}} = V_{\text{total}}$.

With a given a , let $U_{\text{total}} = V_{\text{total}}$ and then the critical load can be obtained by solving the equation group made up of Eqs. (1)–(12) numerically. The obtained critical load varies with a and the minimal value of the critical load is regarded as the final critical load. For the specimen with I-stiffener shown in Fig. 1(a), the solved critical load is $P = 50.2$ kN. The corresponding bending normal stresses on the top and the bottom of the stiffener are 494.9 and 104.98 MPa, respectively. The yield limit

of the material (7B04-T7451) used is 445 MPa, as listed in Table 1. It is obvious that the stiffener top exceeds the yield limit, while the bottom of the stiffener is still in elastic state. Therefore, the assumption that the stiffener is in elastic state is incorrect. The correct stress state of the stiffener is shown in Fig. 3, and the stiffener top is in elastic-plastic state.

For the elastic deformation section where the stress is lower than the initial yield stress, the unit length load is still expressed as $N_x = N_0 \left(\frac{z}{h_1} - 1 \right)$.

For the plastic deformation section, the stress and strain relation in Eq. (4) is no longer correct. The strain ε_{ij} of this section can be divided into two parts: the elastic strain ε_{ij}^e and the plastic strain ε_{ij}^p , and

$$\varepsilon_{ij} = \varepsilon_{ij}^e + \varepsilon_{ij}^p \quad (13)$$

where the elastic strain ε_{ij}^e is still expressed as the same as that in Eq. (4).

In this study, the Mises yield function is adopted to analyze the plastic deformation problems, and the equivalent stress is expressed as:

$$\bar{\sigma} = \sqrt{\sigma_{xx}^2 - 2\sigma_{xx}\sigma_{zz} + \sigma_{zz}^2 + 3\sigma_{xz}^2} \quad (14)$$

where $\bar{\sigma}$ is the equivalent stress. According to Drucker's postulate, it is obtained:

$$d\varepsilon_{ij}^p = d\bar{\varepsilon}^p \frac{\partial \bar{\sigma}}{\partial \sigma_{ij}} \quad (15)$$

where $\bar{\varepsilon}^p$ is the equivalent plastic strain. Under the proportional loading path, it is obtained:

$$\varepsilon_{ij}^p = \bar{\varepsilon}^p \frac{\partial \bar{\sigma}}{\partial \sigma_{ij}} \quad (16)$$

The relation between the equivalent stress and the equivalent plastic strain is expressed as:

$$\bar{\sigma} = h(\bar{\varepsilon}^p) \quad (17)$$

With Eqs. (4), (13), (15) and (16), the relation between the strain and stress in the plastic deformation section can be obtained:

$$\begin{cases} \varepsilon_{xx} = \frac{1}{E}(\sigma_{xx} - \nu\sigma_{zz}) + \bar{\varepsilon}^p \frac{\partial \bar{\sigma}}{\partial \sigma_{xx}} \\ \varepsilon_{zz} = \frac{1}{E}(\sigma_{zz} - \nu\sigma_{xx}) + \bar{\varepsilon}^p \frac{\partial \bar{\sigma}}{\partial \sigma_{zz}} \\ \gamma_{xz} = \frac{1}{G}\sigma_{xz} + \bar{\varepsilon}^p \frac{\partial \bar{\sigma}}{\partial \sigma_{xz}} \end{cases} \quad (18)$$

From Eqs. (14) and (18), it is obtained:

$$\begin{cases} \sigma_{xx} = \frac{1}{2} \left(\frac{E(\varepsilon_{xx} + \varepsilon_{zz})}{1-\nu} + \frac{\varepsilon_{xx} - \varepsilon_{zz}}{\frac{1+\nu}{E} + \frac{2\bar{\varepsilon}^p}{\bar{\sigma}}} \right) \\ \sigma_{zz} = \frac{1}{2} \left(\frac{E(\varepsilon_{xx} + \varepsilon_{zz})}{1-\nu} - \frac{\varepsilon_{xx} - \varepsilon_{zz}}{\frac{1+\nu}{E} + \frac{2\bar{\varepsilon}^p}{\bar{\sigma}}} \right) \\ \sigma_{xz} = \frac{G\bar{\sigma}\gamma_{xz}}{3G\bar{\varepsilon}^p + \bar{\sigma}} \end{cases} \quad (19)$$

The internal energy of the stiffener can be obtained by integrating the elastic and the plastic section. For the elastic deformation section [11],

$$V_{\text{elastic}} = \frac{1}{2} \int_0^a \int_0^{h_2} \int_{-\frac{b}{2}}^{\frac{b}{2}} (\sigma_{xx}\varepsilon_{xx} + \sigma_{zz}\varepsilon_{zz} + \tau_{xz}\gamma_{xz}) dx dz dy \quad (20)$$

where h_2 is the coordinate of the boundary between the elastic and the plastic section in z direction. From Eqs. (3)–(4), it is obtained:

$$V_{\text{elastic}} = \frac{D}{2} \int_0^a \int_0^{h_2} \left\{ (\nabla^2 \omega)^2 - 2(1-\nu) \left[\frac{\partial^2 \omega}{\partial x^2} \frac{\partial^2 \omega}{\partial z^2} - \left(\frac{\partial^2 \omega}{\partial x \partial z} \right)^2 \right] \right\} dx dz \quad (21)$$

For the plastic deformation section, it is obtained:

$$V_{\text{plastic}} = \frac{1}{2} \int_0^a \int_{h_2}^h \int_{-b/2}^{b/2} (\sigma_{xx}\varepsilon_{xx} + \sigma_{zz}\varepsilon_{zz} + \tau_{xz}\gamma_{xz}) dx dz dy \quad (22)$$

From Eqs. (3), (18) and (19), it is obtained:

$$\begin{aligned} V_{\text{plastic}} = & \frac{b^3}{24} \int_0^a \int_{h_2}^h \frac{2E}{1-\nu} \left(\left(\frac{\partial^2 \omega}{\partial x^2} \right)^2 + \left(\frac{\partial^2 \omega}{\partial z^2} \right)^2 + \right. \\ & \left. 2 \frac{\partial^2 \omega}{\partial x^2} \frac{\partial^2 \omega}{\partial z^2} \right) dx dz + \frac{b^3}{24} \int_0^a \int_{h_2}^h \left(\left(\frac{\partial^2 \omega}{\partial x^2} \right)^2 + \right. \\ & \left. \left(\frac{\partial^2 \omega}{\partial z^2} \right)^2 - 2 \frac{\partial^2 \omega}{\partial x^2} \frac{\partial^2 \omega}{\partial z^2} \right) / \left(\frac{1+\nu}{E} + \frac{2\bar{\varepsilon}^p}{\bar{\sigma}} \right) dx dz + \\ & \frac{b^3}{12(1+\nu)} \int_0^a \int_{h_2}^h \left(\frac{\partial^2 \omega}{\partial x \partial z} \right)^2 \frac{\bar{\sigma}}{3G\bar{\varepsilon}^p + \bar{\sigma}} dx dz \end{aligned} \quad (23)$$

The relation between the stress and coordinate can be obtained from Eqs. (3) and (19). In order to simplify the computing process, $\bar{\sigma} = h(\bar{\varepsilon}^p)$ is assumed to be a linear function and the parameters can be solved with the uniaxial tensile test data.

With a given a , the strain energy V_{plastic} of the plastic deformation section can be obtained from Eq. (23), and then the total strain energy V_{total} can be obtained. With the total work of the external load (as expressed in Eq. (10)), the critical buckling load can be solved on the basis of energy method in which $U_{\text{total}}=V_{\text{total}}$. Based on the above method, a series of critical loads can be solved with different a values.

The relation between a and the critical load of the specimen with I-stiffener is shown in Fig. 4. It can be seen that the critical load varies with a , when a is very small, the selected part of the stiffener is unlikely to buckle due to its geometric shape, and the obtained critical load is very large; when a is very large, the stiffener is also unlikely to buckle because the stress on the surfaces is very small, and the obtained critical load is also very large; when a is a special value, the critical load may reach the minimum value which is regarded as the final critical load.

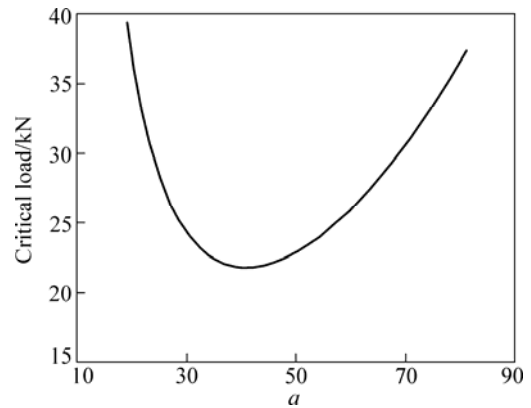


Fig. 4 Theoretical relationship between a value and critical buckling load

The theoretical critical buckling load of the specimen with I-stiffener calculated by the above method is 21.84 kN and the experimental critical buckling load is 20.06 kN, which means that the calculated critical load can reasonably reflect the actual situation. The buckling load predicted by theoretical method is a little larger than that measured in the experiment. The measure errors in the experiments and the simplification in the theoretical analysis lead to the error between the theoretical and the experimental results. After the critical buckling load is obtained, the corresponding critical punch displacement can be obtained from elastic-plastic mechanics method or from simulated load-displacement curves of the press bend experiment.

3.2 Critical buckling load of specimens with other cross section shapes

The critical buckling loads (or punch displacements)

of the specimen with T-stiffener can be solved by the above method. In the press bending of the specimens with multi-stiffener, if the stress state of each stiffener is similar to that of the specimens with single stiffener, the specimen can be first decomposed to a group of specimens with different single stiffeners and then they can be solved respectively. The minimum value of the critical buckling loads (or the displacement of the punch) is adopted to be the final critical value.

As for the crosswise stiffened specimen, the punch always applies load to the intersections of the stiffeners, and the buckling peak no longer appears at the loading position of the punch, as shown in Fig. 2(b). The above mentioned method can be also used just by removing the work of load P from the total work of the external force.

4 Conclusions

1) The stress analysis of the press bend process is carried out with mechanical and numerical method. It is found that the top and bottom of the specimen in the press bending are under elastic-plastic and elastic loading conditions, respectively.

2) The method for solving the critical buckling load (or punch displacement) on the stiffeners in the aluminum alloy integral panel based on energy method is proposed. The relation between the length of the assumed section that buckles first on the whole stiffener and the resulting critical buckling load is presented, then the critical load is determined. Besides the specimen with I-stiffener, the proposed method is also used for solving the critical load of other specimens with single stiffener and the specimens with multi-stiffener.

3) The press bend experiments of the specimen with I-stiffener and crosswise stiffened specimen are performed. It is found that the predicted results based on the proposed method agree well with the experimental results.

4) With the proposed method, the buckling of the stiffeners in the press bend forming of aluminium alloy integral panels with high-stiffener can be predicted reasonably.

References

- [1] MUNROE J, WILKINS K, GRUBER M. Integral airframe structures (IAS)—Validated feasibility study of integrally stiffened metallic fuselage panels for reducing manufacturing costs [R]. NASA/CR-2000-209337. Seattle, Washington: Boeing Commercial Airplane Group, 2000.
- [2] YAN Yu, WAN Min, WANG Hai-bo. FEM equivalent model for press bend forming of aircraft integral panel [J]. Transactions of Nonferrous Metals Society of China, 2009, 19(2): 414–424.
- [3] YAN Yu, WAN Min, WANG Hai-bo, HUANG Lin. Design and optimization of press bend forming path for producing aircraft integral panels with compound curvatures [J]. Chinese Journal of Aeronautics, 2010, 23(2): 274–282.
- [4] YAN Yu. Forming modeling and path optimization technology for press bending of aluminum alloy high-stiffener integral panel [D]. Beijing: School of Mechanical Engineering and Automation, Beihang University, 2009: 60–66. (in Chinese)
- [5] YORK C B, WILLIAMS F W. Aircraft wing panel buckling analysis: Efficiency by approximations [J]. Computers and Structures, 1998, 68: 665–676.
- [6] GAL E, LEVY R, ABRAMOVICH H, PAVSNER P. Buckling analysis of composite panels [J]. Composite-Structures, 2006, 73(21): 179–185.
- [7] MATTHIAS H, PETER H. A new analysis model for the effective stiffness of stiffened metallic panels under combined compression and shear stress [J]. Aerospace Science and Technology, 2006, 10(4): 316–326.
- [8] DEGENHARDT R, KLING A, ROHWER, K, ORIFICI A C, THOMSON R S. Design and analysis of stiffened composite panels including post-buckling and collapse [J]. Computers and Structures, 2008, 86(9): 919–929.
- [9] LIU Jin-song. Incremental forming and self-adapting control on integral panel skin with grid-type ribs [D]. Shenyang: Institute of Metal, Chinese Academy of Science, 2004: 27–68. (in Chinese)
- [10] REN Li-mei, WANG Zhong-tang, LIU Jin-song, ZHANG Shi-hong. Analysis and numerical simulation on stability in irregular section of ribs bending process [J]. Journal of Plasticity Engineering, 2003, 10(5): 39–41. (in Chinese)
- [11] LIANG Bing-wen, HU Shi-guang. Stability theory of elasto-plasticity [M]. Beijing: National Defence Industry Press, 1983: 108–147. (in Chinese)
- [12] NEMETH M P. Buckling of long compression-loaded anisotropic plates restrained against inplane lateral and shear deformations [J]. Thin-Walled Structures, 2004, 42: 639–685.
- [13] ATHIANNAN K, PALANINATHAN R. Buckling of cylindrical shells under transverse shear [J]. Thin-Walled Structures, 2004, 42: 1307–1328.
- [14] JABERZADEH E, AZHARI M. Elastic and inelastic local buckling of stiffened plates subjected to non-uniform compression using the Galerkin method [J]. Applied Mathematical Modelling, 2009, 33(4): 1874–1885.
- [15] KUMAR S P, RAMACHANDRA L S. Buckling of rectangular plates with various boundary conditions loaded by non-uniform inplane loads [J]. International Journal of Mechanical Sciences, 2010, 52(6): 819–828.
- [16] XIAO Ming-xin. Instability theory of plate [M]. Chengdu: Sichuan Science and Technology Press, 1993: 61–80. (in Chinese)

整体壁板压弯成形中的筋条失稳预测

阎 昱¹, 王海波¹, 万 敏²

1. 北方工业大学 机电工程学院, 北京 100144;

2. 北京航空航天大学 机械工程及自动化学院, 北京 100191

摘 要: 为实现对整体壁板压弯成形中筋条失稳的预测, 基于能量法、弹塑性力学和数值解析提出压弯成形过程中筋条临界失稳载荷的求解方法。在设计的压弯模具上进行压弯失稳试验。结果表明, 基于本文提出的方法所得的理论临界失稳载荷与试验结果吻合较好。采用本文所提出的方法可以对铝合金高筋整体壁板压弯成形中的筋条失稳问题进行合理地预测。

关键词: 压弯成形; 失稳预测; 整体壁板

(Edited by FANG Jing-hua)